The Use of (*E*)- and (*Z*)-Phosphoenol-3-fluoropyruvate as Mechanistic Probes Reveals Significant Differences between the Active Sites of KDO8P and DAHP Synthases†

Cristina M. Furdui,‡ Apurba K. Sau,‡ Orit Yaniv,§ Valery Belakhov,§ Ronald W. Woodard,|| Timor Baasov,§ and Karen S. Anderson*,‡

Department of Pharmacology, Yale University School of Medicine, 333 Cedar Street, New Haven, Connecticut 06520-8066, Department of Chemistry and Institute of Catalysis, Science and Technology, Technion, Haifa 32000, Israel, and Department of Medicinal Chemistry and Chemistry, University of Michigan, Ann Arbor, Michigan 48109-1065

Received December 27, 2004; Revised Manuscript Received March 15, 2005

ABSTRACT: The enzymes 3-deoxy-D-*manno*-2-octulosonate-8-phosphate (KDO8P) synthase and 3-deoxy-D-*arabino*-2-heptulosonate-7-phosphate (DAHP) synthase catalyze a similar aldol-type condensation between phosphoenolpyruvate (PEP) and the corresponding aldose: arabinose 5-phosphate (A5P) and erythrose 4-phosphate (E4P), respectively. While KDO8P synthase is metal-dependent in one class of organisms and metal-independent in another, only a metal-dependent class of DAHP synthases has thus far been identified in nature. We have used catalytically active *E* and *Z* isomers of phosphoenol-3-fluoropyruvate [(*E*)- and (*Z*)-FPEP, respectively] as mechanistic probes to characterize the differences and/or the similarities between the metal-dependent and metal-independent KDO8P synthases as well as between the metal-dependent KDO8P synthase and DAHP synthase. The direct evidence of the overall stereochemistry of the metal-dependent *Aquifex pyrophilus* KDO8P synthase (*Ap*KDO8PS) reaction was obtained by using (*E*)- and (*Z*)-FPEPs as alternative substrates and by subsequent ^{19}F NMR analysis of the products. The results reveal the *si* face addition of the PEP to the *re* face of the carbonyl of A5P, and establish that the stereochemistry of *Ap*KDO8PS is identical to that of the metal-independent *Escherichia coli* KDO8P synthase enzyme (*Ec*KDO8PS). In addition, both *Ap*KDO8PS and *Ec*KDO8PS enzymes exhibit high selectivity for (*E*)-FPEP versus (*Z*)-FPEP, the relative k_{cat}/K_m ratios being 100 and 33, respectively. In contrast, DAHP synthase does not discriminate between (*E*)- and (*Z*)-FPEP (the k_{cat}/K_m being $\sim 7 \times 10^{-3}$ μM^{-1} s^{-1} for both compounds). The pre-steady-state burst experiments for *Ec*KDO8PS showed that product release is rate-limiting for the reactions performed with either PEP, (*E*)-FPEP, or (*Z*)-FPEP, although the rate constants, for both product formation and product release, were lower for the fluorinated analogues than for PEP [125 and 2.3 s^{-1} for PEP, 2.5 and 0.2 s^{-1} for (*E*)-FPEP, and 9 and 0.1 s^{-1} for (*Z*)-FPEP, respectively]. The observed data indicate substantial differences in the PEP subsites and open the opportunity for the design of selective inhibitors against these two families of enzymes.

Many of today's clinical drugs, ranging from structure-based enzyme inhibitors to mechanism-based inhibitors, take advantage of the unique chemical properties of fluorine (*1*, *2*). However, the detailed molecular mechanism that constitutes the basis of the activity of fluorinated compounds has only recently started to be addressed (*3*). In this paper, the *E* and *Z* isomers of phosphoenol-3-fluoropyruvate [(*E*)- and (*Z*)-FPEP,[1] respectively] were used to probe the active sites and the reaction mechanism of two phosphoenolpyruvate (PEP)-dependent enzymes, 3-deoxy-D-*manno*-2-octulosonate-8-phosphate synthase (KDO8PS, EC 4.1.2.16) and 3-deoxy-D-*arabino*-2-heptulosonate-7-phosphate synthase (DAHPS, EC 4.1.2.15).

KDO8PS and DAHPS represent two important targets in the design of new antibiotics. DAHPS catalyzes the first committed step in the biosynthesis of three essential aromatic amino acids (Tyr, Trp, and Phe) and other aromatic metabolites in microorganisms and plants (*4*−*8*). Mammals do not possess this biosynthetic pathway, and its inhibition will be deleterious to bacteria, affecting both Gram-negative and Gram-positive organisms. KDO8PS is present in Gram-negative bacteria (*9*, *10*) and in some plants (*5*, *11*), and is involved in the biosynthesis of lipopolysaccharides, an essential component of the bacterial cell wall, responsible for both cell survival and cell virulence (*12*, *13*).

† This work was supported by NIH Grants GM 61413 and GM 71805 (K.S.A.) and the U.S.-Israel Binational Science Foundation (Grant 2002-126) to T.B. and K.S.A.

* To whom correspondence should be addressed. Phone: (203) 785-4526. Fax: (203) 785-7670. E-mail: karen.anderson@yale.edu.

‡ Yale University School of Medicine.

§ Technion.

|| University of Michigan.

[1] Abbreviations: KDO8P, 3-deoxy-D-*manno*-2-octulosonate 8-phosphate; PEP, phosphoenolpyruvate; A5P, D-arabinose 5-phosphate; (*E*)-FPEP, (*E*)-phosphoenol-3-fluoropyruvate; (*Z*)-FPEP, (*Z*)-phosphoenol-3-fluoropyruvate; DAHPS, 3-deoxy-D-*arabino*-2-heptulosonate-7-phosphate synthase; *Ec*KDO8PS, *E. coli* KDO8P synthase; *Ap*KDO8PS, *A. pyrophilus* KDO8P synthase; TEAB, triethylammonium bicarbonate; TCA, trichloroacetic acid.

10.1021/bi047282q CCC: $30.25
Published on Web 04/22/2005

Scheme 1: Net Aldol Reactions Catalyzed by KDO8PS (a) and DAHPS (b)

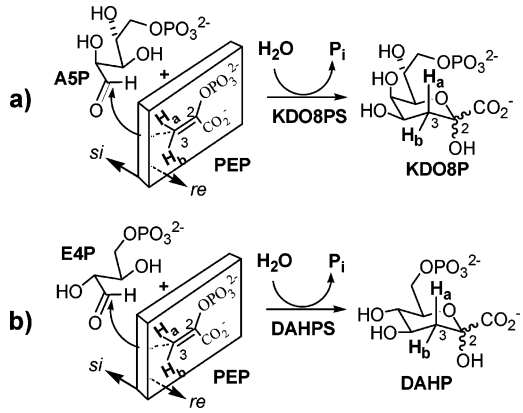

KDO8PS and DAHPS share several structural (*14*−*17*) and mechanistic (*17*−*26*) characteristics by catalyzing very similar condensation reactions between PEP and the corresponding aldose: the five-carbon sugar D-arabinose 5-phosphate (A5P) in KDO8PS and the four-carbon sugar D-erythrose 4-phosphate (E4P) in DAHPS. Both reactions produce inorganic phosphate (P_i) and unusual 3-deoxyulosonic acids: an eight-carbon sugar KDO8P and a seven-carbon sugar DAHP, as illustrated in parts a and b of Scheme 1, respectively. Despite these similarities, while all the bacterial and eukaryotic DAHPSs require divalent metal ions for activity, two different classes of KDO8PSs have been recognized with respect to their requirement for metals (*27*, *28*). *Aquifex pyrophilus* KDO8PS [*Ap*KDO8PS (*27*, *29*)] and *Escherichia coli* DAHPS [*Ec*DAHPS (*7*)] are both metal-dependent enzymes, with the major difference being the higher thermal stability of *Ap*KDO8PS. However, unlike *Ec*DAHPS, *E. coli* KDO8P synthase (*Ec*KDO8PS) is a metal-independent enzyme catalyzing the same reaction as the *Ap*KDO8PS, a metal-dependent enzyme. With the protein sequence being more than 40% identical in *Ec*KDO8PS and *Ap*KDO8PS enzymes (*27*), and with active site residues almost completely overlapping in an overlay of the structural data (*17*), it should be very difficult to design specific inhibitors that will selectively inhibit one enzyme while leaving the other unaffected. Moreover, despite the low level of sequence similarity between *Ec*KDO8P and *Ec*DAHP (<5% identical) (*9*), the crystal structures of these proteins reveal a high level of similarity at the level of active site structure. The work described herein was aimed at finding subtle differences between the active sites of these enzymes, which could then be exploited in the design of more selective inhibitors.

(*Z*)-FPEP [and later (*E*)-FPEP] was widely used as an alternate substrate to probe the stereochemical course of different PEP-utilizing enzyme reactions (*30*). Phosphoenolpyruvate carboxykinase, enolase, and pyruvate phosphate dikinase showed absolute stereospecificity for the *Z* isomer (*30*, *31*), although the specificity constants for (*Z*)-FPEP were up to 350-fold lower than that for PEP. Pyruvate kinase was able to use both isomers, although it had higher specificity for (*Z*)-FPEP (*30*).

Using NMR, (*E*)- and (*Z*)-FPEP have also been investigated as alternative substrates of the *Ec*DAHPS (*32*) and *Ec*KDO8PS enzymes (*20*, *32*). These studies were indeed instrumental in determining the overall stereochemistry of both enzymes. The *si* face of PEP is directed to react with the *re* face of the carbonyl of the respective aldose (Scheme 1). However, while the NMR data clearly showed that *Ec*DAHPS is able to utilize both isomers with similar rates, *Ec*KDO8PS selectively utilized the (*E*)-FPEP isomer over the (*Z*)-FPEP isomer by a ratio of ~2000 as estimated by calculation of the V_{max} values. Although no kinetic parameters were determined for these reactions and the underlying molecular basis for this difference between the two enzymes is unclear, it is interesting that the observed selectivity of *Ec*KDO8PS for (*E*)-FPEP is in contrast to the majority of PEP-utilizing enzymes, which show either absolute specificity or a stronger preference for (*Z*)-FPEP. In addition, while the stereochemistry of both metal-dependent *Ec*DAHPS and metal-independent *Ec*KDO8PS has been established, no such studies on the stereochemistry of metal-dependent *Ap*KDO8PS have yet been performed.

A combination of steady-state and pre-steady-state experiments was applied to probe the active sites of *Ec*DAHPS, *Ec*KDO8PS, and *Ap*KDO8PS reactions with respect to their reactivity toward fluorinated substrate analogues of PEP. The determination of the overall stereochemistry of the *Ap*KDO8PS-catalyzed reaction is also reported. The data provide important information about the interactions between fluorinated substrates and the enzymes, suggesting substantial differences in the PEP-binding sites between KDO8PS and DAHPS enzymes.

EXPERIMENTAL PROCEDURES

Materials and Methods. Phosphoenolpyruvate potassium salt (PEP), arabinose 5-phosphate disodium salt (A5P), manganese chloride, magnesium chloride, adenosine 5′-triphosphate, potassium monophosphate, ammonium chloride, inorganic pyrophosphatase, and triethylamine were purchased from Sigma. [1-^{14}C]Pyruvate and [1-^{14}C]arabinose were obtained from American Radiolabeled Chemicals, and the HPLC Mono Q 5/5 anion-exchange column was from Amersham Biosciences.

Spectrophotometric measurements were taken on a Hewlett-Packard 8452A diode array spectrophotometer using 1 cm path length cells with a thermostated cell holder, and a circulating water bath at the desired temperature. ^{19}F NMR spectra were recorded on a Bruker WH-200 spectrometer operating at 188.313 MHz and are referenced externally to trifluoroacetic acid at −77.0 ppm.

[1-^{14}C]PEP Synthesis. Radiolabeled PEP was enzymatically synthesized from [1-^{14}C]pyruvate (American Radiolabeled Chemicals) by coupling pyruvate phosphate dikinase (PPDK), obtained as a generous gift from D. Dunaway-Mariano, to the inorganic pyrophosphatase reaction. After purification by Q-Sepharose anion-exchange chromatography using a 20 mM to 1 M triethylammonium bicarbonate (TEAB) gradient, the fractions containing PEP were pooled and lyophilized. Final stock solutions (5.6 mM) contained 29 300 dpm/nmol.

[^{32}P]A5P Synthesis. Radiolabeled A5P was enzymatically synthesized from D-arabinose (3 mg/mL) using hexokinase (50 mg/mL) and [γ-^{32}P]ATP (6.2 mg/mL, 0.5 mCi/mL) in 50 mM Tris (pH 7.5). The radiolabeled A5P was purified by Q-Sepharose anion-exchange chromatography using a 20

to 500 mM TEAB gradient. The fractions containing A5P were pooled and lyophilized. The A5P was dissolved in 50 mM Tris (pH 7.5) at a final concentration of 1 mM with 100 000 dpm/nmol.

[1-^{14}C]A5P Synthesis. [1-^{14}C]A5P (3 mCi/mmol) was synthesized enzymatically by using hexokinase (20 mg/mL) and [1-^{14}C]arabinose (4 mCi/mmol, ICN) in 50 mM Hepes (pH 7.6). The radiolabeled A5P was purified with a Q-Sepharose column (Amersham Pharmacia) using a linear gradient of 20 mM to 1 M TEAB (pH 8.0). The fractions containing radiolabeled A5P were pooled and lyophilized. The lyophilized powder was dissolved in 50 mM Hepes (pH 7.6) to a final concentration of 2.3 mM.

Purification of EcKDO8PS. The *Ec*KDO8PS was expressed and purified following the reported procedure (*28*) with some modifications. The concentration of the enzyme was determined using the Bradford assay kit (Bio-Rad), which then normalized to an extinction coefficient ϵ of 15,219 mM^{-1} cm^{-1} at 280 nm.

Preparation of PEP-Free EcKDO8PS. Previous studies have shown that *Ec*KDO8PS was isolated with 1 equiv of tightly bound PEP (*25*). To make the PEP-free enzyme, 400 μM *Ec*KDO8PS was incubated with cold A5P (the concentration of A5P was kept 1.5 times higher than the enzyme concentration), and the mixture was kept at 4 °C for ~1 h. To ensure all the PEP is removed from the enzyme, a small amount of the reaction mixture was incubated with [1-^{14}C]-A5P and the mixture then subjected to HPLC. No radiolabeled KDO8P peak was found in the HPLC analysis. The mixture was then dialyzed against two changes of 4 L of 50 mM Tris-HCl (pH 7.5) at 4 °C. The reaction mixture was passed through a Bio-spin 6 column (Bio-Rad). A small amount of the reaction mixture was incubated with [1-^{14}C]-PEP, and the mixture was subjected to HPLC. No radiolabeled KDO8P peak was found in the HPLC analysis. This suggests that the enzyme is free from both bound PEP and excess A5P. To remove excess A5P from the reaction mixture, we found it necessary to use both dialysis and the spin column. This suggests that excess A5P binds also very tightly to the PEP-free enzyme.

*Purification of ApKDO8PS. Ap*KDO8PS was purified as previously reported (*27*). The protein concentration was routinely determined by using an extinction coefficient for KDO8PS at 280 nm of 43.2 mM^{-1} cm^{-1}. However, the catalytic rates were calculated on the basis of the active site concentration determined from the burst experiments. The active site concentration was calculated as described in Data Analysis.

*Purification of EcDAHPS. Ec*DAHPS was purified as previously reported (*33*). The protein concentration was determined by using an extinction coefficient for *Ec*DAHPS at 280 nm of 40.5 mM^{-1} cm^{-1}. However, the catalytic rates were calculated on the basis of the active site concentration determined from burst experiments. The active site concentration was calculated as described in Data Analysis and based on the amplitude of the burst.

Preparation of (E)- and (Z)-FPEP. (*E*)- and (*Z*)-FPEP have been synthesized and purified as described by Duffy and Nowak (*31*) with the following minor modifications. The tripotassium salt of (*Z*)-FPEP (50 mg) was photoisomerized at 254 nm (Rayonet photochemical reactor) in a quartz cuvette for 3 h to yield an approximately 70:30 *E*/*Z* mixture. Progress of the reaction was monitored by ^{19}F and ^{31}P NMR. The resulted mixture was purified through the ion-exchange column of Dowex 1X8 (Cl^- form), eluting with a linear gradient of dilute HCl (from 0.02 to 0.1 M). Fractions were analyzed for inorganic phosphate after digestion with $HClO_4$. (*Z*)-FPEP was eluted first (from 0.062 to 0.071 M HCl) followed by (*E*)-FPEP (from 0.075 to 0.089 M HCl). The active fractions were combined and concentrated under reduced pressure. The residues were separately dissolved in water, and the pH of each was carefully adjusted to 7.5 with dilute KOH. The resulting solutions were lyophilized to give pure tripotassium salts of (*E*)-FPEP (32 mg, 64%) and (*Z*)-FPEP (12 mg, 36%). The ^{1}H and ^{19}F NMR data of the products were in agreement with the literature (*34*).

HPLC Analysis of (E)- and (Z)-FPEP. Fifteen nanomoles of PEP, 30 nmol of (*E*)-FPEP, and 15 nmol of (*Z*)-FPEP were injected into a HPLC anion-exchange Mono Q HR 5/5 column on-line with an UV−vis detector set at 225 nm followed by a Flo-One radioactivity detector (Packard Instruments, Downers Grove, IL). The elution conditions were identical to the conditions described in the next section. As an internal standard, we added 1 nmol of [1-^{14}C]PEP in the PEP and (*Z*)-FPEP samples and 2 nmol of [1-^{14}C]PEP in the (*E*)-FPEP sample. The UV−vis detector showed different retention times for PEP (15.9 min), (*Z*)-FPEP (15.6 min), and (*E*)-FPEP (16.3 min). [1-^{14}C]PEP had the same retention time in all three samples as shown by the radioactivity detector (16.4 min). There is a 0.5 min delay between the UV−vis and radioactivity detector as established by co-injection of cold and radiolabeled PEP standards.

Determination of the Extinction Coefficient for PEP, (E)-FPEP, and (Z)-FPEP. The classical approach of measuring the extinction coefficient for a compound is to plot the absorbance at a certain wavelength versus the concentration of the compound. According to the Lambert−Beer law, the extinction coefficient is determined by fitting the data to a linear equation where the slope represents the extinction coefficient. However, this procedure is contingent on the compound purity besides other factors (e.g., pH for some compounds). The presence of impurities that might have absorption at the same wavelength as the compound of interest results in an erroneous value for the extinction coefficient. Therefore, we chose a different approach to determine the extinction coefficients for (*E*)- and (*Z*)-FPEP. The experiments were performed using *Ap*KDO8PS at 60 °C. In one experiment, we determined the catalytic rates of *Ap*KDO8PS by using a radioactive assay with [^{32}P]A5P and following the formation of [^{32}P]KDO8P, [^{32}P]-(3*R*)-[3F]-KDO8P, and [^{32}P]-(3*S*)-[3F]KDO8P when the reactions were performed in the presence of PEP, (*E*)-FPEP, and (*Z*)-FPEP, respectively. The reaction mixture contained 390 nM KDO8P synthase, 120 μM [^{32}P]A5P, 200 μM $MnCl_2$, and either PEP (400 μM), (*E*)-FPEP (33.7 μM), or (*Z*)-FPEP (500 μM) in 50 mM Tris (pH 7.5). At different time points, 50 μL aliquots were removed and the reactions quenched with 50 μL of 0.5 M EDTA. The quenched reaction mixture was then diluted 4-fold to bring the EDTA concentration to 60 mM; 60 μL was removed and analyzed by HPLC with an on-line UV−vis detector (Waters 486 Tunable Absorbance Detector) and a flow scintillation analyzer for radioactivity detection (Perkin-Elmer, Downers Grove, IL). The analysis system was automated using a Waters (Milford, MA) 717plus autosam-

pler. The substrates and products were separated on an anion-exchange Mono Q HR 5/5 column (Pharmacia, Piscataway, NJ) using a 35 min linear TEAB gradient from 20 mM to 1 M. The elution was performed with a flow rate of 1 mL/min. Before entering the radioactivity detector, the eluent was mixed with liquid scintillation cocktail (Monoflow V, National Diagnostics) at a flow rate of 5 mL/min. Under these conditions, the retention times for [^{32}P]A5P and [^{32}P]-KDO8P were 10.2 and 12.7 min, respectively. However, while the retention time of (3*S*)-[3F]KDO8P was 12.5 min, the retention time of (3*R*)-[3F]KDO8P was 14.9 min. This assay is independent of the extinction coefficient of the substrate, and as such, the reaction rates determined from this assay were used as the true rates. The determined catalytic rates were 6.2 s^{-1} for PEP, 0.35 s^{-1} for (*E*)-FPEP, and 0.77 s^{-1} for (*Z*)-FPEP. Using the same concentrations of substrates and enzyme, the reactions were followed with a continuous spectrophotometric assay. The consumption of PEP, (*E*)-FPEP, or (*Z*)-FPEP was monitored at 232 and 225 nm. Using previously determined catalytic rates and the measured absorbancies in these experiments, the extinction coefficients for PEP, (*E*)-FPEP, and (*Z*)-FPEP were determined from eq 1.

Steady-State Assays. EcKDO8PS. The steady-state kinetic experiments for *Ec*KDO8PS activity were performed by monitoring the consumption of PEP, (*E*)-FPEP, and (*Z*)-FPEP at 232 or 225 nm. For all experiments, initial rates for the decrease in the absorbance of PEP, (*E*)-FPEP, and (*Z*)-FPEP were measured by varying the concentrations of their respective substrates, while the concentration of A5P was kept constant at saturation level. To maintain a saturating level of A5P, experiments were performed at 200 μM A5P (K_m of A5P $\sim$ 39 μM). The concentration of the enzyme was kept at 300 nM. The initial rate was calculated from a linear least-squares fit of the initial decrease in absorbance. As expected, the experimental data under the conditions described above were observed to follow typical Michaelis−Menten kinetics, and the apparent Michaelis constant (K_m) and maximum velocity (k_{cat}) were determined.

ApKDO8PS. To determine the steady-state kinetic parameters of (*E*)-FPEP, (*Z*)-FPEP, and PEP, we followed the dependence of the catalytic rate on the concentration of these compounds. The reaction mixture contained 1 mM A5P, 200 μM $MnCl_2$, and 300 nM KDO8P synthase in 1 mL of 50 mM Tris (pH 7.5). The concentration of PEP and PEP analogues was varied, and the decrease in absorbance at 225 nm was followed in a continuous UV−vis spectrophotometric assay. The steady-state catalytic rate was calculated using the initial rate (OD/s) and the extinction coefficient of PEP, (*E*)-FPEP, and (*Z*)-FPEP determined as described above.

Establishing the Stereochemistry of the ApKDO8PS-Catalyzed Reaction. In attempts to determine the overall stereochemistry of the *Ap*KDO8PS-catalyzed reaction, stereospecifically labeled samples of FPEP were prepared (as described above) and used as alternative substrates for *Ap*KDO8PS. The enzymatic reactions were performed separately with the purified samples of (*Z*)- and (*E*)-FPEP isomers and with the *Z*/*E* mixture, and the progress of reactions was monitored by ^{19}F NMR. The reaction products were isolated, and the exact configuration at the C3 center was unambiguously assigned by NMR analysis. The reaction mixture typically contained Tris-acetate buffer (0.1 M, pH 6.5), EDTA (0.2 mM), $CdCl_2$ (0.5 mM), A5P (0.1 M), FPEP (0.04 M), *Ap*KDO8PS ($\sim$3−30 μM), and 50% D_2O for lock. The reaction was performed at 60 °C, and after consumption of all the fluorinated substrate (determined by ^{19}F NMR), the resulting mixture was purified through an ion-exchange column of AG 1X8 (100−200 mesh, HCO_3^- form), eluting with a linear gradient (from 0.1 to 0.6 M) of TEAB buffer (pH 7.5). Fractions were analyzed for inorganic phosphate after digestion with $HClO_4$. The active fractions were combined and concentrated under reduced pressure. The residue was dissolved in water and passed over the short column of Dowex 50W (K^+ form). Active fractions were combined and lyophilized to give the pure tripotassium salt of the product.

EcDAHPS. As in the steady-state experiments described above, for the *E. coli* DAHP synthase the reaction mixture contained 80 nM DAHP synthase, 200 μM $MnCl_2$, and 500 μM E4P in 50 mM Tris (pH 7.5). The concentration of PEP and PEP analogues was varied, and the decrease in absorbance at 225 nm was followed in a continuous UV−vis spectrophotometric assay. For the fluorinated PEP analogues, nonsaturating kinetics was observed. A further increase in substrate concentration was not possible because of the high absorbance values which rendered the measurements inaccurate.

Rapid Chemical Quench Experiments. Rapid quench experiments were performed using a Kintek RFQ-3 Rapid Chemical Quench (Kintek Instruments, Austin, TX). The reaction was initiated by mixing the enzyme solution (15 μL) with the radiolabeled substrate (15 μL). In all cases, the concentrations of the enzyme and substrates cited in the text are those after mixing and during the reaction. The reaction was then quenched with 67 μL of 0.6 N KOH. For fluorinated PEP analogues, it was found that the products (3*S*)- and (3*R*)-[3F]KDO8P were not stable in KOH. Hence, the reaction was quenched with 67 μL of triethylamine, and the products were found to be stable under these conditions. The reaction mixture was mixed with 100 μL of $CHCl_3$, and the aqueous layer was collected. The substrates and products were separated and quantified using the anion-exchange column coupled with simultaneous radioactivity detection. The HPLC separation was performed on a Mono Q HR 5/5 anion-exchange column with flow rate of 1 mL/min. A gradient separation was employed using solvent A [20 mM TEAB (pH 9.0)] and solvent B [1 M TEAB (pH 9.0)]. A linear gradient program was as follows: from 100 to 0% A from 0 to 35 min and from 0 to 100% B from 0 to 35 min, followed by re-equilibration. The retention times were 10.2 (A5P), 12.7 (KDO8P), 12.5 [(3*S*)-[3F]KDO8P], and 14.9 min [(3*R*)-[3F]KDO8P]. During the HPLC analysis, a small amount of cold PEP was always injected as an internal standard as it coelutes with hot PEP and its elution time can be monitored at 232 nm by the absorbance detector. These conditions were used to analyze the samples generated from the rapid chemical quench experiments.

Data Analysis. Extinction Coefficients for PEP, (E)-FPEP, and (Z)-FPEP. The extinction coefficients (mM^{-1} cm^{-1}) were determined using eq 1

$$\epsilon = v_1/(cv_2) \quad (1)$$

in which v_1 (OD/s) represents the initial velocity at 225 nm

in the UV−vis assay, c (mM) represents the concentration of KDO8P synthase in the UV−vis assay, and v_2 (s^{-1}) represents the catalytic rate determined using the radiolabeled [^{32}P]A5P.

Steady-State Experiments. Data were fit to the Michaelis−Menten equation, and the k_{cat} and K_m parameters for PEP, (*E*)-FPEP, and (*Z*)-FPEP were determined.

Pre-Steady-State Burst Experiments. The formation of KDO8P, (3*R*)-[3F]KDO8P, and (3*S*)-[3F]KDO8P (μM) was plotted against time (s), and data were fitted to a single-exponential equation followed by a linear equation.

$$C = C_0(1 - e^{-k_1 t}) + C_0 k_2 t \quad (2)$$

where C represents the product concentration at time t, amplitude C_0 corresponds to the active site concentration, k_1 is the rate constant for product formation (s^{-1}), and k_2 is the rate of product release (s^{-1}). The percentage of active enzyme can be calculated by dividing C_0 by the enzyme concentration. Data were analyzed using Kaleidagraph version 3.52 (Synergy Software, Reading, PA).

RESULTS

Enzyme Assay Development for PEP and FPEP Substrates. To facilitate the steady-state kinetic analysis of KDO8PS and DAHPS reactions with fluorinated analogues of PEP, our efforts were initially directed toward elaborating an accurate assay procedure. To the best of our knowledge, there are only two reports in the literature on the extinction coefficient of (*Z*)-FPEP. Initially, this value was reported to be 1.28 mM^{-1} cm^{-1} (*30*) at 240 nm [50 mM imidazole-HCl (pH 6.8)]. Later, Pilch et al. reported values of 0.58 mM^{-1} cm^{-1} at 240 nm and 1.54 mM^{-1} cm^{-1} at 230 nm [50 mM phosphate buffer (pH 6.7)] (*35*). Although there were differences in the experimental conditions used by the two groups, these cannot account for the large difference in the determined values. The extinction coefficient of (*E*)-FPEP has not yet been reported.

As described in Experimental Procedures, the extinction coefficients for PEP and FPEP were determined using a combination of continuous spectrophotometric and discontinuous radiolabeled assays. At 232 nm, the extinction coefficient measured for PEP was 2.84 mM^{-1} cm^{-1}, which is identical to the value reported in the literature (*22*). At 225 nm, the extinction coefficients of PEP, (*E*)-FPEP, and (*Z*)-FPEP were determined to be 3.63, 2.96, and 0.67 mM^{-1} cm^{-1}, respectively.

HPLC Analysis of PEP, (E)-FPEP, and (Z)-FPEP. Surprisingly, when the samples from the radioactive assay described in the previous section were analyzed by HPLC, we became aware of different retention times for [^{32}P]-(3*R*)-3-fluoro-KDO8P, [^{32}P]KDO8P, and [^{32}P]-(3*S*)-3-fluoro-KDO8P (Figure 1). To investigate if the effect extends to the substrates for the reaction, we determined the retention times for PEP, (*E*)-FPEP, and (*Z*)-FPEP by HPLC using the same chromatographic conditions as in the experiment described above. The wavelength for the absorbance detector was set at 225 nm. To ensure that all the chromatographic runs were identical, we added as a control trace amounts of [1-^{14}C]PEP in the samples containing cold PEP, (*E*)-FPEP, and (*Z*)-FPEP (Figure 2). The results showed that the three compounds have different retention times, the order of elution

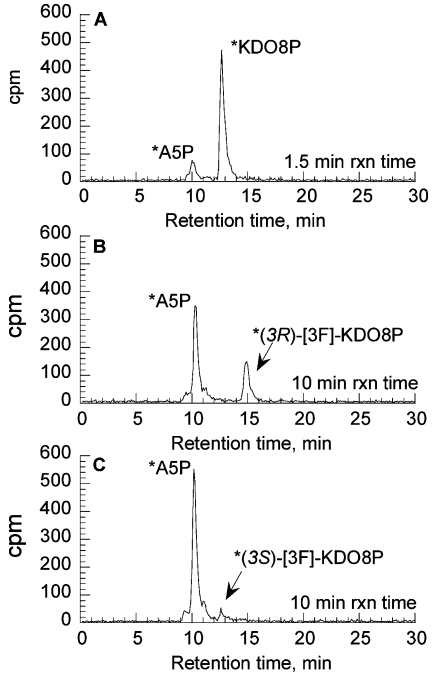

FIGURE 1: HPLC analysis of the reaction products from the *Ap*KDO8P synthase reaction. Representative chromatograms from the KDO8P synthase discontinuous assay using radiolabeled [^{32}P]-A5P are presented: (A) 1.5 min time point of the reaction of radiolabeled [^{32}P]A5P with PEP, (B) 10 min time point of the reaction of radiolabeled [^{32}P]A5P with (*E*)-FPEP, and (C) 10 min time point of the reaction of radiolabeled [^{32}P]A5P with (*Z*)-FPEP. Different retention times for KDO8P (12.7 min) and (3*S*)- and (3*R*)-[3F]KDO8P (14.9 and 12.5 min, respectively) could be observed.

being (*Z*)-FPEP (15.6 min), PEP (15.9 min), and then (*E*)-FPEP (16.3 min). In all three runs, the retention time for [1-^{14}C]PEP was 16.4 min. This observation was applied in developing a simpler separation procedure for the FPEP isomers by ion-exchange chromatography, as described in Experimental Procedures.

The fact that the mixture of PEP, (*E*)-FPEP, and (*Z*)-FPEP can be separated by anion-exchange chromatography indicates that the position of the fluorine atom in *E* or *Z* geometry changes the electronic properties of PEP so that (*E*)-FPEP is more negatively charged than PEP and (*Z*)-FPEP is least negatively charged. This may result from small differences in the intramolecular structures of PEP and its fluorinated analogues due to electrostatic repulsions between the fluorine and the negatively charged phosphate and carboxylate groups (N. Adir, personal communication).

Steady-State Kinetic Parameters for EcKDO8PS, ApKDO8PS, and EcDAHPS. The steady-state kinetic parameters were determined for the *Ec*KDO8PS, *Ap*KDO8PS, and *Ec*DAHPS reactions with PEP and with its two 3-fluoro analogues. The data for *Ap*KDO8PS are presented in Figure 3, and the results are summarized in Table 1. The same relative specificity for the three compounds is observed for both *A. pyrophilus* and *E. coli* KDO8P synthase. In the case of *Ap*KDO8P synthase, although the k_{cat}/K_m for (*E*)-FPEP (0.21 μM^{-1} s^{-1}) is only slightly lower than that for PEP (0.34 μM^{-1} s^{-1}), the enzyme clearly shows a lower specificity for (*Z*)-FPEP (0.0022 μM^{-1} s^{-1}). For the *Ec*KDO8P synthase, the k_{cat}/K_m for (*E*)-FPEP is ~3 times lower than that for PEP. However, the k_{cat}/K_m value for (*Z*)-FPEP is much lower than that for PEP or (*E*)-FPEP (Table 1), following the same trend

Table 1: Steady-State Kinetic Parameters for *Ap*KDO8PS, *Ec*KDO8PS, and *Ec*DAHPS

	*Ap*KDO8PS			*Ec*KDO8PS			*Ec*DAHPS		
	PEP	(*E*)-FPEP	(*Z*)-FPEP	PEP	(*E*)-FPEP	(*Z*)-FPEP	PEP[a]	(*E*)-FPEP	(*Z*)-FPEP
k_{cat} (s^{-1})	9 ± 0.2	1 ± 0.1	1.1 ± 0.02	4.5 ± 0.2	0.5 ± 0.05	0.3 ± 0.04	32	−	−
K_m (μM)	26 ± 1.3	4.7 ± 0.3	500 ± 60	5 ± 0.05	1.9 ± 0.3	32 ± 9	9	−	−
k_{cat}/K_m (μM^{-1} s^{-1})	0.3	0.2	0.002	0.9	0.3	0.009	3.55	0.0069	0.007

[a] The parameters are from ref *38*.

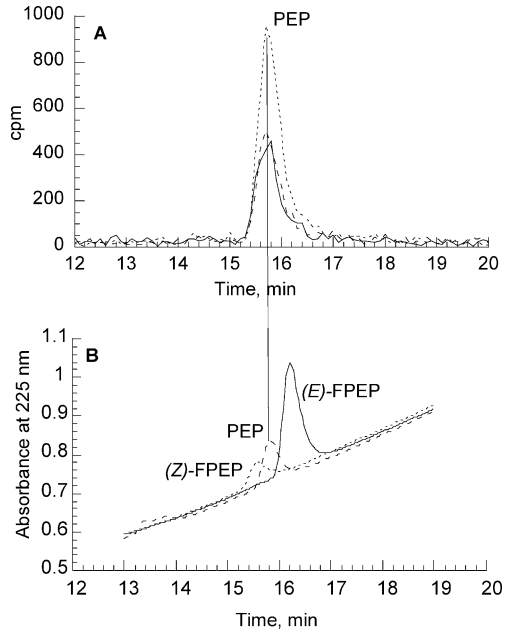

FIGURE 2: HPLC analysis of PEP, (*E*)-FPEP, and (*Z*)-FPEP. PEP (15 nmol), (*E*)-FPEP (30 nmol), and (*Z*)-FPEP (15 nmol) were injected in a HPLC anion-exchange Mono-Q column on-line with an UV−vis detector set at 225 nm followed by a radioactivity detector. As an internal standard, 1 nmol of [^{14}C]PEP was added in each sample with the exception of (*E*)-FPEP, where 2 nmol of [^{14}C]PEP was added. PEP and the fluoro-PEP analogues were eluted with a linear gradient of 20 mM to 1 M TEAB buffer at pH 8.0 as described in Experimental Procedures. The UV−vis detector showed different retention times for PEP (15.9 min), (*Z*)-FPEP (15.6 min), and (*E*)-FPEP (16.3 min) (B), while [1-^{14}C]PEP had the same retention time in all three samples as shown with the radioactivity detector (16.4 min) (A).

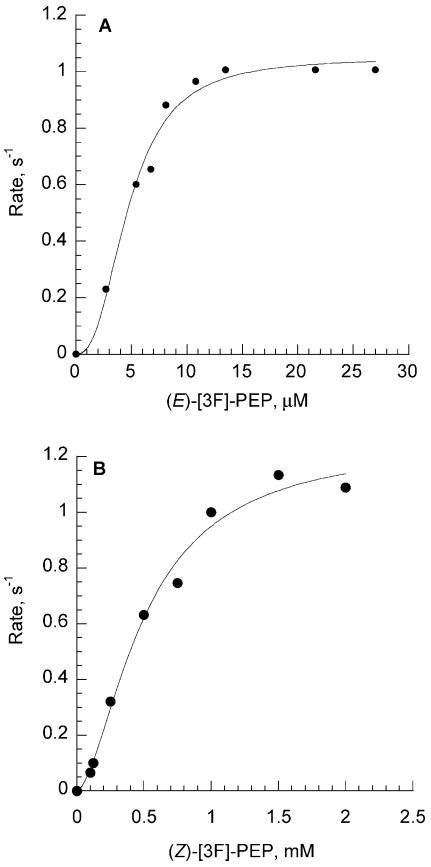

FIGURE 3: Steady-state assays for *A. pyrophilus* KDO8P synthase. The reaction mixture contained A5P (1 mM), $MnCl_2$ (200 μM), and KDO8P synthase (300 nM) in 1 mL of 50 mM Tris (pH 7.5). The reaction was performed at 60 °C. The concentration of (*E*)-FPEP (A) and (*Z*)-FPEP (B) was varied, and the decrease in absorbance at 225 nm was followed in a continuous UV−vis spectrophotometric assay. The steady-state catalytic rate was calculated using the initial rate (OD/s) and the extinction coefficients of (*E*)-FPEP (2.96 mM^{-1} cm^{-1}) and (*Z*)-FPEP (0.67 mM^{-1} cm^{-1}).

as the *Ap*KDO8P synthase. On the other hand, the *Ec*DAHP synthase does not seem to distinguish between the two fluorinated isomers, with k_{cat}/K_m values for both (*E*)- and (*Z*)-FPEP being 7×10^{-3} μM^{-1} s^{-1} (Figure 4). In the case of *E. coli* DAHP synthase, the very low reaction rate coupled with the high absorbance at higher enzyme and substrate concentrations precluded an accurate determination of the k_{cat} or K_m parameters. According to basic Michaelis−Menten kinetics, at low substrate concentrations the k_{obs} (normalized by enzyme concentration, s^{-1}) is linearly dependent on substrate concentration and the slope corresponds to k_{cat}/K_m. Therefore, in this case, the k_{cat}/K_m values for the two FPEP isomers are reported and were determined from the linear slope at low substrate concentrations (Figure 4).

Stereochemistry of the ApKDO8PS-Catalyzed Reaction. To establish the stereochemistry of the *Ap*KDO8PS-catalyzed reaction, we have carried out separate enzymatic reactions with *Z* and *E* isomers of FPEP. Incubation of (*Z*)-FPEP (>95% stereochemically pure) with *Ap*KDO8PS and monitoring the reaction progress by ^{19}F NMR showed the gradual consumption of the substrate at −139.5 ppm and the subsequent appearance of four signals centered at −201.9, −204.9, −208.0, and −211.8 ppm (data not shown). The same four signals were recorded for the clean product isolated after purification of the reaction mixture by ion-exchange chromatography (Figure 5a). These signals were assigned to the tautomeric mixture of (3*S*)-[3F]KDO8P (fluorine atom oriented in an axial position), like those reported for the *Ec*KDO8PS-catalyzed reaction in the presence of (*Z*)-FPEP (*20*).

When the similar experiment with *Ap*KDO8PS was carried out in the presence of (*E*)-FPEP (>95% stereochemically pure, −150.4 ppm), the reaction was much faster and the appearance of only two new signals was detected. The same two signals with the same relative intensities (−187.8 and −206.1 ppm, with relative intensities of 5 and 95%, respectively), corresponding to the major α-furanose and

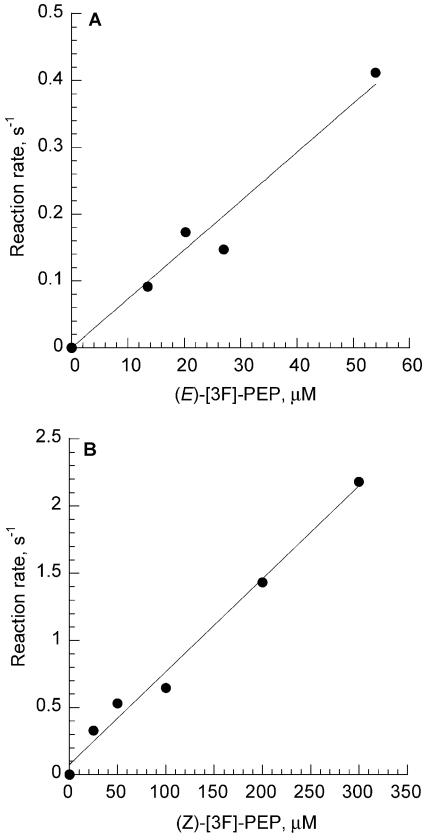

FIGURE 4: Steady-state assays for *E. coli* DAHP synthase. The reaction mixture contained E4P (1 mM), $MnCl_2$ (200 μM), and DAHP synthase (300 nM) in 1 mL of 50 mM Tris (pH 7.5). The reaction was performed at 25 °C. The concentration of (*E*)-FPEP (A) and (*Z*)-FPEP (B) was varied, and the decrease in absorbance at 225 nm was followed in a continuous UV−vis spectrophotometric assay. The steady-state catalytic rate was calculated using the initial rate (OD/s) and the extinction coefficients of (*E*)-FPEP (2.96 mM^{-1} cm^{-1}) and (*Z*)-FPEP (0.67 mM^{-1} cm^{-1}). The k_{cat}/K_m for (*Z*)-FPEP was 6.9×10^{-3} μM^{-1} s^{-1} and for (*E*)-FPEP was 7×10^{-3} μM^{-1} s^{-1}.

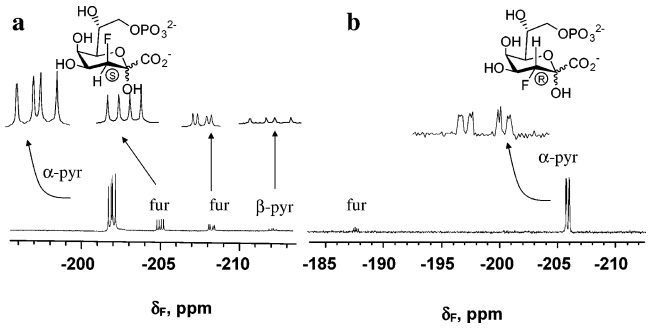

FIGURE 5: ^{19}F NMR spectra of (a) (3*S*)-[3-F]KDO8P and (b) (3*R*)-[3-F]KDO8P.

α-pyranose forms of (3*R*)-[3F]KDO8P (fluorine atom oriented in an equatorial position) (*20*), were recorded for the purified product as illustrated in Figure 5b. Thus, the results indicate that the overall reaction catalyzed by *Ap*KDO8PS is stereospecific with respect to C3 of PEP. Since (*Z*)-FPEP gave rise to (3*S*)-[3F]KDO8P and (*E*)-FPEP produced the opposite 3*R* diastereomer of [3F]KDO8P, this observation dictates that the attachment of C3 of PEP to the carbonyl of A5P must proceed from the *si* face of the enzyme-bound PEP, identical to that of the metal-independent *Ec*KDO8PS-catalyzed reaction (Scheme 1a).

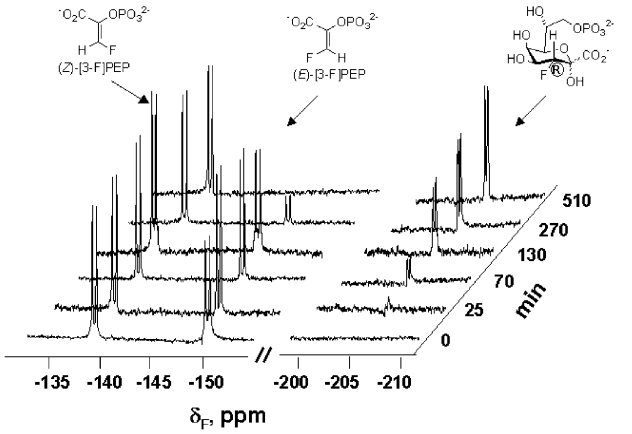

FIGURE 6: Time course of ^{19}F NMR spectra showing the conversion of (*E*)-FPEP to (3*R*)-[3-F]KDO8P in the presence of Tris-acetate buffer (0.1 M, pH 6.5), 0.2 mM EDTA, 0.5 mM $CdCl_2$, A5P (0.109 M), a *Z*/*E* mixture of [3-F]PEP (0.044 M, 1:1 ratio), *Ap*KDO8PS (2.75 μM), and 50% D_2O for lock. The enzymatic reactions were carried out for 510 min at 60 °C. Spectra were acquired on a Bruker WH-200 instrument operating at 188.313 MHz and are referenced externally to TFA (at −77.0 ppm). Insets are the corresponding structural assignments.

To further illustrate the stereochemical preference of *Ap*KDO8PS for (*E*)-FPEP, a similar experiment was carried out with the *Z*/*E* mixture (∼1:1) of FPEP (Figure 6). At short time intervals, the consumption of only (*E*)-FPEP was observed, very similar to that for the previously reported *Ec*KDO8PS-catalyzed reaction (*32*). Thus, in contrast to different requirements for metals for catalytic activity, both *Ec*KDO8PS and *Ap*KDO8PS show the same overall stereospecificity with respect to PEP and similar a stereochemical preference for (*E*)-FPEP over (*Z*)-FPEP. On the other hand, however, although both *Ap*KDO8PS and *Ec*DAHPS require divalent metals for full catalytic performance, *Ec*DAHPS does not seem to discriminate between the two isomers of FPEP, suggesting subtle differences in the PEP active sites of these two enzymes.

Pre-Steady-State Burst Experiments for E. coli KDO8P Synthase. To determine the active site concentration of *E. coli* KDO8P synthase, we have carried out a pre-steady-state burst experiment using radiolabeled [1-^{14}C]A5P as a substrate. A representative burst experiment of the native enzyme showing the time course for biphasic formation of [^{14}C]-KDO8P is shown in Figure 7A. The rate of product formation was 125 s^{-1} for the fast phase and 2.3 s^{-1} for the slower linear phase. The amplitude of the burst experiment shown in Figure 7 provides an estimate of active site concentration which was determined to be approximately 85%. The biphasic behavior of the burst curve indicates that the product release is at least the rate-limiting step of the reaction. The results are consistent with previous pre-steady-state burst experiments performed with this enzyme (*23*).

Pre-Steady-State Burst Experiments of the PEP-Free Enzyme with Fluoro-PEP Analogues Using Radiolabeled [1-^{14}C]A5P. Panels B and C of Figure 7 show the burst of products (3*S*)-[3F]KDO8P and (3*R*)-[3F]KDO8P in the presence of 0.82 mM (*Z*)-FPEP and 1.1 mM (*E*)-FPEP, respectively. In both cases, biphasic product formation was observed. The data were fitted to a burst equation (eq 2), yielding rate constants for the fast phase of 9 and 2.5 s^{-1} for *Z* and *E* isomers, respectively. The rate constants for

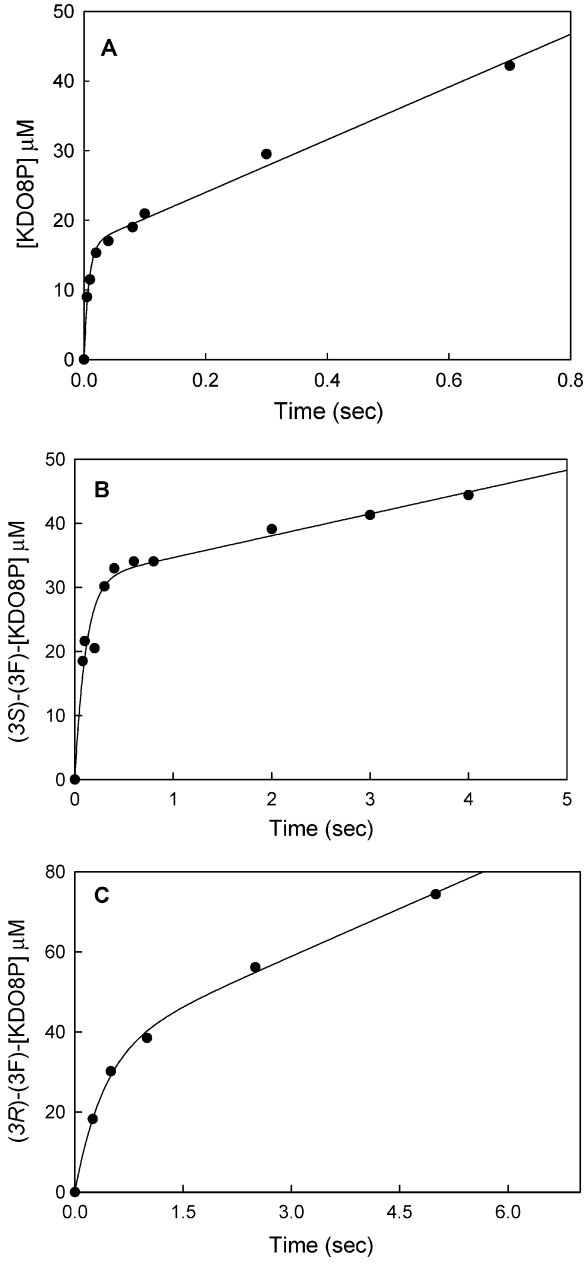

FIGURE 7: Pre-steady-state burst experiments for *E. coli* KDO8P synthase. (A) A solution containing enzyme (19 μM) preincubated with [^{14}C]A5P (61.3 μM) was mixed with PEP (250 μM) at 25 °C (final concentration after mixing). The reaction was terminated by quenching it with 0.4 N KOH, and the formation of product, KDO8P, was monitored by HPLC with radioactive detection. The curve represents a fit to a burst equation with a rate of 125 s^{-1} for the fast phase and a rate of 2.3 s^{-1} for the slower phase. (B) A solution containing enzyme (77.8 μM) preincubated with [^{14}C]A5P (99.6 μM) was mixed with (*Z*)-FPEP (0.82 mM) at 25 °C (final concentration after mixing). The curve represents a fit to a burst equation with a rate of 9 s^{-1} for the fast phase and a rate of 0.1 s^{-1} for the slower phase. (C) A solution containing enzyme (37.5 μM) preincubated with [^{14}C]A5P (100 μM) was mixed with (*E*)-FPEP (1.1 mM) at 25 °C (final concentration after mixing). The curve represents a fit to a burst equation with a rate of 2.5 s^{-1} for the fast phase and a rate of 0.2 s^{-1} for the slower phase. In panels B and C, the reaction was terminated by quenching with Et_3N, and the solution was mixed with $CHCl_3$. The aqueous layer was collected, and formation of the product was monitored by HPLC with radioactive detection.

product release (0.2 and 0.3 s^{-1} for *Z* and *E* isomers, respectively) were in agreement with the steady-state rate determined from the spectrophotometric measurements (see Table 1).

DISCUSSION

As described in the introductory section, *Ap*KDO8PS, *Ec*KDO8PS, and *Ec*DAHPS catalyze the condensation reaction of PEP with A5P or E4P. Despite the fact that *Ap*KDO8PS and *Ec*DAHPS are metal-dependent, *Ec*KDO8PS is metal-independent, or *Ec*KDO8P synthase is mesophilic while *Ap*KDO8PS is thermophilic, the steady-state kinetic parameters with the natural substrates are relatively similar (Table 1). To better understand the differences and/or similarities between these enzymes, the stereospecifically labeled analogues of the PEP substrate with the fluorine atom, (*Z*)-FPEP and (*E*)-FPEP, were employed as mechanistic probes. Earlier NMR experiments showed that *Ec*KDO8PS and *Ec*DAHPS have different reactivities toward these two compounds. While *Ec*KDO8PS prefers (*E*)-FPEP over (*Z*)-FPEP, *Ec*DAHPS does not seem to discriminate between the two isomers (*32*). Our interest has been in determining if the differences arise from the presence or absence of metal or from the protein structure itself. Therefore, a stereochemical analysis of the metal-dependent *Ap*KDO8PS-catalyzed reaction, along with a detailed kinetic analysis of the (*E*)- and (*Z*)-FPEP reactivity with respect to the three enzymes, has been performed.

The results obtained in this study establish for the first time that the overall stereochemistry of *Ap*KDO8P is identical to that of *Ec*KDO8P: the *si* face of PEP and the *re* face of the carbonyl of A5P. In addition, it was also shown that even though there are different requirements for metals, both *Ap*KDO8P and *Ec*KDO8P show a similar preference for (*E*)-FPEP over (*Z*)-FPEP. This more efficient utilization of (*E*)-FPEP by the KDO8PS enzymes is dissimilar, however, from that of *Ec*DAHPS, which showed no discrimination between the two isomers of FPEP. The detailed kinetic analysis of these enzymes with the FPEPs provided some reasonable explanation for these observations.

First, the lack of an accurate extinction coefficient for (*E*)-FPEP and (*Z*)-FPEP and the instability of the reaction products, the corresponding (3*R*)-[3F]KDO8P and (3*S*)-[3F]-KDO8P, under the conventional quenching conditions were the limiting factors in the comparative kinetic analysis of this reaction. By examining different quenching materials and conditions, we determined a specific set of quenching conditions under which (3*R*)-[3F]KDO8P and (3*S*)-[3F]-KDO8P were stable. In addition, by using a combination of biochemical techniques, we determined the extinction coefficients for both (*E*)- and (*Z*)-FPEP. The data facilitated the monitoring of both substrate decay and product formation under steady-state or pre-steady-state conditions. At 225 nm, the extinction coefficient of PEP is slightly larger than that of (*E*)-FPEP and significantly higher than that of (*Z*)-FPEP. There does not seem to be a correlation between the extinction coefficients and the retention times of the three compounds on the anion-exchange HPLC column, the order of elution being (*Z*)-FPEP, then PEP, and then (*E*)-FPEP. The retention times of the three compounds on the HPLC column suggest that there is a difference in the negative charge present on the molecule with (*E*)-FPEP being more negatively charged than (*Z*)-FPEP. Interestingly, this in-

creased negative charge on the *E* isomer versus the *Z* isomer is further reflected in the chemical shift difference of the fluorine atom in these two isomers. As seen from Figure 6, the resonance of (*Z*)-FPEP (−139.5 ppm) is significantly deshielded from that of (*E*)-FPEP (−150.4 ppm), indicating that the ground-state charge at C3 of (*Z*)-FPEP is more positive than that of (*E*)-FPEP. The higher net negative charge of (*E*)-FPEP should influence the potency of binding to the positively charged residues in the active site of the enzyme, making its association much tighter than that of (*Z*)-FPEP. Also, the higher negative charge density at C3 of (*E*)-FPEP makes this stereoisomer a better nucleophile (Scheme 1).

Theoretical analysis of the chemical reactivity of C3 of PEP through density functional theory suggested that the enzyme controls this atom's reactivity by controlling the dihedral angle between the carboxylate and the C═C bond of PEP (*36*). The ionization state of PEP was also shown to play an important role in its reactivity. Thus, the observed different reactivities of (*E*)-FPEP and (*Z*)-FPEP with different enzymes suggest that the interaction of an enzyme with PEP or with its analogues should be a crucial factor that determines the reactivity of these compounds.

How are these different electronic properties of PEP, (*E*)-FPEP, and (*Z*)-FPEP correlating with the chemical reactivity in *Ap*KDO8PS, *Ec*KDO8PS, and *Ec*DAHPS? The steady-state kinetic parameters summarized in Table 1 point to the ground-state destabilization (determined by K_m) as the main component in lowering the transition-state energy for KDO8P synthase catalysis. Even more, the relative kinetic parameters for both the metallo- and non-metallo-KDO8P synthase are strikingly similar, suggesting that the metal is not involved in determining the stereospecificity of this reaction. We propose that at least in the case of KDO8P synthase, there is a fine-tuning of the energy the enzyme is spending to move the substrate into a conformation that enables maximum reactivity of C3 and that the organizational entropy plays the determinant role in ground-state destabilization. This hypothesis is supported by the crystal structure of the *Aquifex aeolicus* KDO8PS−PEP binary complex which shows a 10° twist between the PEP carboxylate plane and the enol plane (*17*). It is not unreasonable to expect that the energy necessary to twist the carboxylate plane relative to the enol plane is different from PEP to (*Z*)-FPEP and (*E*)-FPEP. While the different electronic properties mentioned above for (*Z*)-FPEP and (*E*)-FPEP in solution might be different from that when they are bound to enzyme, it is clear that the magnitude of the dihedral angle in the enzyme-bound form will determine the final charge on C3 of these compounds and subsequently their reactivity in the aldol condensation step.

The burst experiments suggest that C3 of (*Z*)-FPEP is more reactive than C3 of (*E*)-FPEP and ~14-fold less reactive than PEP. We are currently working on determining the crystal structure of *Ap*KDO8PS in the presence of (*E*)- and (*Z*)-FPEP, which will shed light on the reaction pathway these enzymes employ to accomplish the catalysis. The available X-ray structures of the *E. coli* and *Aquifex aeolicus* KDO8P synthases in complex with a bisubstrate inhibitor that mimics the linear reaction intermediate enzyme showed a dissimilar arrangement of the inhibitor molecule in the active site (*26*, *37*). This is stressing the fact that the subtle difference in the active sites of these two enzymes can cause very different binding of the inhibitor molecule despite the similar K_i values for the two enzyme species (3.3 and 7 μM for the *E. coli* and *A. aeolicus* KDO8P synthases, respectively) (*24*, *26*). The data presented in this paper further indicate that such differences could arise from the PEP subsite. To target specific bacterial strains, one needs to develop specific inhibitors targeted to unique proteins (present in only one of the strains and absent in humans) or exploit subtle differences in the active site of the same target protein in the two species. While the active sites of the enzymes studied here are highly conserved, our studies show that it is possible to discriminate between these species with inhibitors directed toward the PEP binding site.

In summary, this work provides the first detailed kinetic analysis of the reactivity of (*E*)- and (*Z*)-FPEP with both metallo- and non-metallo-KDO8PS as well as with the phylogenetically related metalloenzyme *Ec*DAHPS. By determining the extinction coefficients of (*E*)- and (*Z*)-FPEP and by finding the appropriate quenching conditions for the reaction, we were able to determine both the steady-state and pre-steady-state kinetic parameters for the KDO8PS-catalyzed reaction with these compounds. It was found that the three enzymes have different stereoselectivity and stereospecificity toward the two fluorinated compounds and that the protein interaction with the fluorinated isomers is the major determinant of the rate of product formation. These reveal subtle differences between the active sites of *Ap*KDO8PS, *Ec*KDO8PS, and *Ec*DAHPS, which may be utilized as a design feature in the development of specific inhibitors against each of the three enzymes.

REFERENCES

1. Walsh, C. T. (1984) Suicide substrates, mechanism-based enzyme inactivators: Recent developments, *Annu. Rev. Biochem. 53*, 493−535.
2. Wirsching, P., and O'Leary, M. H. (1988) (Z)-3-(Fluoromethyl)-phosphoenolpyruvate: Synthesis and enzymatic studies, *Biochemistry 27*, 1348−1355.
3. Olsen, A. J., Banner, D. W., Seiler, P., O., S. U., D'Arcy, A., Stihle, M., Muller, K., and Diederich, F. (2003) *Angew. Chem., Int. Ed. 42*, 2507−2511.
4. Bracher, M., and Schweingruber, E. (1977) Purification of the tyrosine inhibi-deoxy-D-*arabino*-heptulosonate-7-phosphate synthase from *Schizosaccharomyces pombe*, *Biochim. Biophys. Acta 485*, 446−451.
5. Gorlach, J., Schmid, J., and Amrhein, N. (1994) Abundance of transcripts specific for genes encoding enzymes of the prechorismate pathway in different organs of tomato (*Lycopersicon esculentum L.*) plants, *Planta 193*, 216−223.
6. Paravicini, G., Schmidheini, T., and Braus, G. (1989) Purification and properties of the 3-deoxy-D-*arabino*-heptulosonate-7-phosphate synthase (phenylalanine-inhibitable) of *Saccharomyces cerevisiae*, *Eur. J. Biochem. 186*, 361−366.
7. Staub, M., and Denes, G. (1969) Purification and properties of the 3-deoxy-D-*arabino*-heptulosonate-7-phosphate synthase (phenylalanine sensitive) of *Escherichia coli* K12. II. Inhibition of activity of the enzyme with phenylalanine and functional group-specific reagents, *Biochim. Biophys. Acta 178*, 599−608.
8. Wu, J., Howe, D. L., and Woodard, R. W. (2003) *Thermotoga maritima* 3-deoxy-D-*arabino*-heptulosonate-7-phosphate synthase: The ancestral eubacterial DAHP synthase? *J. Biol. Chem. 278*, 27525−27531.
9. Birck, M. R., and Woodard, R. W. (2001) *Aquifex aeolicus* 3-deoxy-D-manno-2-octulosonic acid 8-phosphate synthase: A new class of KDO 8-P synthase? *J. Mol. Evol. 52*, 205−214.
10. Jensen, R. A., Xie, G., Calhoun, D. H., and Bonner, C. A. (2002) The correct phylogenetic relationship of KdsA (3-deoxy-D-*manno*-octulosonate 8-phosphate synthase) with one of two independently

evolved classes of AroA (3-deoxy-D-*arabino*-heptulosonate 7-phosphate synthase), *J. Mol. Evol. 54*, 416−423.
11. Delmas, F., Petit, J., Joubes, J., Seveno, M., Paccalet, T., Hernould, M., Lerouge, P., Mouras, A., and Chevalier, C. (2003) The gene expression and enzyme activity of plant 3-deoxy-D-manno-2-octulosonic acid-8-phosphate synthase are preferentially associated with cell division in a cell cycle-dependent manner, *Plant Physiol. 133*, 348−360.
12. Clements, J. M., Coignard, F., Johnson, I., Chandler, S., Palan, S., Waller, A., Wijkmans, J., and Hunter, M. G. (2002) Antibacterial activities and characterization of novel inhibitors of LpxC, *Antimicrob. Agents Chemother. 46*, 1793−1799.
13. Jackman, J. E., Fierke, C. A., Tumey, L. N., Pirrung, M., Uchiyama, T., Tahir, S. H., Hindsgaul, O., and Raetz, C. R. (2000) Antibacterial agents that target lipid A biosynthesis in Gram-negative bacteria. Inhibition of diverse UDP-3-O-(r-3-hydroxymyristoyl)-n-acetylglucosamine deacetylases by substrate analogs containing zinc binding motifs, *J. Biol. Chem. 275*, 11002−11009.
14. Radaev, S., Dastidar, P., Patel, M., Woodard, R. W., and Gatti, D. L. (2000) Structure and mechanism of 3-deoxy-D-*manno*-octulosonate 8-phosphate synthase, *J. Biol. Chem. 275*, 9476−9484.
15. Wagner, T., Kretsinger, R. H., Bauerle, R., and Tolbert, W. D. (2000) 3-Deoxy-D-*manno*-octulosonate-8-phosphate synthase from *Escherichia coli*. Model of binding of phosphoenolpyruvate and D-arabinose-5-phosphate, *J. Mol. Biol. 301*, 233−238.
16. Wang, J., Duewel, H. S., Stuckey, J. A., Woodard, R. W., and Gatti, D. L. (2002) Function of His185 in *Aquifex aeolicus* 3-deoxy-D-*manno*-octulosonate 8-phosphate synthase, *J. Mol. Biol. 324*, 205−214.
17. Duewel, H. S., Radaev, S., Wang, J., Woodard, R. W., and Gatti, D. L. (2001) Substrate and metal complexes of 3-deoxy-D-*manno*-octulosonate-8-phosphate synthase from *Aquifex aeolicus* at 1.9 Å resolution. Implications for the condensation mechanism, *J. Biol. Chem. 276*, 8393−8402.
18. Hedstrom, L., and Abeles, R. (1988) 3-Deoxy-D-*manno*-octulosonate-8-phosphate synthase catalyzes the C−O bond cleavage of phosphoenolpyruvate, *Biochem. Biophys. Res. Commun. 157*, 816−820.
19. Dotson, G. D., Dua, R. K., Clemens, J. C., Wooten, E. W., and Woodard, R. W. (1995) Overproduction and one-step purification of *Escherichia coli* 3-deoxy-D-*manno*-octulosonic acid 8-phosphate synthase and oxygen transfer studies during catalysis using isotopic-shifted heteronuclear NMR, *J. Biol. Chem. 270*, 13698−13705.
20. Kohen, A., Berkovich, R., Belakhov, V., and Baasov, T. (1993) Stereochemistry of the KDO8P synthase. An efficient synthesis of the 3-fluoro analogues of KDO8P, *Bioorg. Med. Chem. Lett. 3*, 1577−1582.
21. Dotson, G. D., Nanjappan, P., Reily, M. D., and Woodard, R. W. (1993) Stereochemistry of 3-deoxyoctulosonate 8-phosphate synthase, *Biochemistry 32*, 12392−12397.
22. Kohen, A., Jakob, A., and Baasov, T. (1992) Mechanistic studies of 3-deoxy-D-*manno*-2-octulosonate-8-phosphate synthase from *Escherichia coli*, *Eur. J. Biochem. 208*, 443−449.
23. Liang, P. H., Lewis, J., Anderson, K. S., Kohen, A., D'Souza, F. W., Benenson, Y., and Baasov, T. (1998) Catalytic mechanism of Kdo8P synthase: Transient kinetic studies and evaluation of a putative reaction intermediate, *Biochemistry 37*, 16390−16399.
24. Du, S., Faiger, H., Belakhov, V., and Baasov, T. (1999) Towards the development of novel antibiotics: Synthesis and evaluation of a mechanism-based inhibitor of Kdo8P synthase, *Bioorg. Med. Chem. 7*, 2671−2682.
25. Li, Z., Sau, A. K., Shen, S., Whitehouse, C., Baasov, T., and Anderson, K. S. (2003) A snapshot of enzyme catalysis using electrospray ionization mass spectrometry, *J. Am. Chem. Soc. 125*, 9938−9939.
26. Wang, J., Duewel, H. S., Woodard, R. W., and Gatti, D. L. (2001) Structures of *Aquifex aeolicus* KDO8P synthase in complex with R5P and PEP, and with a bisubstrate inhibitor: Role of active site water in catalysis, *Biochemistry 40*, 15676−15683.
27. Shulami, S., Yaniv, O., Rabkin, E., Shoham, Y., and Baasov, T. (2003) Cloning, expression, and biochemical characterization of 3-deoxy-D-*manno*-2-octulosonate-8-phosphate (KDO8P) synthase from the hyperthermophilic bacterium *Aquifex pyrophilus*, *Extremophiles 7*, 471−481.
28. Ray, P. H. (1980) Purification and characterization of 3-deoxy-D-*manno*-octulosonate 8-phosphate synthetase from *Escherichia coli*, *J. Bacteriol. 141*, 635−644.
29. Shulami, S., Furdui, C., Adir, N., Shoham, Y., Anderson, K. S., and Baasov, T. (2004) A reciprocal single mutation affects the metal requirement of KDO8P synthases from *Aquifex pyrophilus* and *Escherichia coli*, *J. Biol. Chem. 279*, 45110−45120.
30. Stubbe, J. A., and Kenyon, G. L. (1972) Analogs of PEP. Substrate specificities of enolase and pyruvate kinase from rabbit muscle, *Biochemistry 11*, 338−345.
31. Duffy, T. H., and Nowak, T. (1984) Stereoselectivity of interaction of phosphoenolpyruvate analogues with various phosphoenolpyruvate-utilizing enzymes, *Biochemistry 23*, 661−670.
32. Sundaram, A. K., and Woodard, R. W. (2000) Probing the stereochemistry of *E. coli* 3-deoxy-D-*arabino*-heptulosonate 7-phosphate synthase (phenylalanine-sensitive)-catalyzed synthesis of KDO 8-P analogues, *J. Org. Chem. 65*, 5891−5897.
33. Sheflyan, G., Howe, D. L., Wilson, T. L., and Woodard, R. W. (1998) Enzymatic Synthesis of 3-deoxy-D-*manno*-octulosonate 8-phosphate, 3-deoxy-D-*altro*-octulosonate 8-phosphate, 3,5-dideoxy-D-*gluco(manno)*-octulosonate 8-phosphate by 3-deoxy-D-*arabino*-heptulosonate 7-phosphate synthase, *J. Am. Chem. Soc. 120*, 11027−11032.
34. Baasov, T., Sheffer-Dee-Noor, S., Kohen, A., Jakob, A., and Belakhov, V. (1993) Catalytic mechanism of 3-deoxy-D-*manno*-2-octulosonate-8-phosphate synthase. The use of synthetic analogues to probe the structure of the putative reaction intermediate, *Eur. J. Biochem. 217*, 991−999.
35. Pilch, P. F., and Somerville, R. L. (1976) Fluorine-containing analogs of intermediates in the shikimate pathway, *Biochemistry 15*, 5315−5320.
36. Li, Y., and Evans, J. N. (1996) The hard−soft acid−base principle in enzymatic catalysis: Dual reactivity of phosphoenolpyruvate, *Proc. Natl. Acad. Sci. U.S.A. 93*, 4612−4616.
37. Asojo, O., Friedman, J., Adir, N., Belakhov, V., Shoham, Y., and Baasov, T. (2001) Crystal structures of KDOP synthase in its binary complexes with the substrate phosphoenolpyruvate and with a mechanism-based inhibitor, *Biochemistry 40*, 6326−6334.
38. Sundaram, A. K., Howe, D. L., Sheflyan, G. Y., and Woodard, R. W. (1998) Probing the potential metal binding site in *Escherichia coli* 3-deoxy-D-*arabino*-heptulosonate 7-phosphate synthase (phenylalanine-sensitive), *FEBS Lett. 441*, 195−199.

BI047282Q